OPTICAL, PHOTOCATALYTIC AND ANTIBACTERIAL PROPERTIES OF ZINC OXIDE NANOPARTICLES OBTAINED BY A SOLVOTHERMAL METHOD

Ludmila MOTELICA[1], Luciana MARINOF[2], Alina HOLBAN[3], Bogdan Stefan VASILE[4], Anton FICAI[5]

Nanocrystalline ZnO powder was prepared by solvothermal method from 1-buthanol at boiling point. The sample was characterized by X-ray diffraction (XRD), transmission electron microscopy (TEM), thermal analysis (TG-DSC), UV-Vis and fluorescence spectra (PL). ZnO is one of the well-known photocatalysts along TiO_2. In each report, it is tested against one pollutant model, and literature data is abundant, but with no possible comparison when different colorants are used. The aim of present study is to compare the photocatalytic properties of ZnO nanoparticles against different colorants used as models for organic pollutants. In this respect, we have used methyl orange, methylene blue, rhodamine B and gentian violet. The strongest photocatalytic activity was found against gentian violet and methyl orange.

The antibacterial activity of ZnO nanoparticles was also tested against Gram-negative and Gram-positive strains Escherichia coli, Staphylococcus aureus, Pseudomonas aeruginosa and Salmonella sp. The best activity was found against Escherichia coli.

Keywords: ZnO, photocatalysis, luminescence, antibacterial activity.

1. Introduction

ZnO is one of the few zinc compounds recognized as safe (GRAS) by the U.S. Food and Drug Administration. Its synthesis is reported in literature by various methods such as thermal decomposition [1], spray pyrolysis [2], solvothermal reaction [3], forced hydrolysis [4], sol-gel method or CVD [5]. ZnO has many applications in various domains like drug delivery [6, 7], cosmetics [8],

[1] PhD student, Dept. of Science and Engineering of Oxide Materials and Nanomaterials, University POLITEHNICA of Bucharest, Romania, e-mail: motelica_ludmila@yahoo.com
[2] Student, Dept. of Inorganic Chemistry, Physical Chemistry and Electrochemistry, University POLITEHNICA of Bucharest, Romania, e-mail: marinof.luciana@yahoo.com
[3] Lector, Dept. of Botany and Microbiology, University of Bucharest, Romania, e-mail: alina_m_h@yahoo.com
[4] CSII, Dept. of Science and Engineering of Oxide Materials and Nanomaterials, University POLITEHNICA of Bucharest, Romania, e-mail: vasile_bogdan_stefan@yahoo.com
[5] Prof., Dept. of Science and Engineering of Oxide Materials and Nanomaterials, University POLITEHNICA of Bucharest, Romania, e-mail: anton.ficai@upb.ro

paints [9], medical devices [10], dentistry [11], textile industry [12] etc. The use of ZnO as sunscreen is not limited to cosmetics [13], but also for rubber or protecting the textile fibers [14-16]. In such applications, the photocatalytic activity must be diminished in order to avoid the degradation of the support material [17-19]. But there are also applications in which a good photocatalytic activity is desirable, like water depollution [20-22], autocleaning films [23] or bacteriostatic applications [24-26].

ZnO effect on epithelialization of wounds and its intrinsic bacteriostatic property promote it as a topical wound dressing in combinations with other substances like chitosan, polylactic acid, cellulose, hydroxyapatite and antibiotics [27-29]. It can also be used in treatment of burns, diaper rashes, blisters, various dermatitis and open skin sores. It has a mild astringent and antibacterial properties and therefore it is used as topical agent in eczema and slight excoriations, in wounds and for hemorrhoids [15]. The antibacterial activity of ZnO is known for some time, but the exact mechanism is still under debate. There are some evidences that the antibacterial activity of ZnO is dependent of size and presence of light, but the data are contradictory regarding which strains are more susceptible: Gram-positive or Gram-negative ones. The presence of light indicates also that the photocatalytic activity might be involved into the promotion of the antibacterial activity [10]. During the light activation, the ZnO nanoparticles are producing reactive oxygen species (ROS) which are responsible of photocatalytic activity but also for oxidative stress which is damaging the bacterial membrane.

The ZnO nanoparticles are proposed to be used as antibacterial agent and UV protective shield in textile industry, especially for clothing. The intrinsic photocatalytic activity of ZnO might be problematic in this kind of applications. It will protect the cotton fibers and colorant from UV degradative action, but in the same time, it can act as a photocatalyst, degrading the material it is supposed to protect. The literature is abundant about the photocatalytic activity of ZnO nanoparticles [2-5], each author reporting the results on one particular colorant used as pollutant model. In this paper, we are reporting for the first time to our knowledge a comparative study of photocatalytic activity on four of the most used colorants: methyl orange, methylene blue, rhodamine B and gentian violet. The results indicate that not all the colorants are susceptible to the photodegradation in same measure. Therefore, it can be useful not only to compare in this way the results reported in literature by different research groups, but it can also help the industry in choosing the best suited dye for antibacterial cloths (e.g. from thiazine class).

Due to the competition of photocatalysis and luminescence associated with the recombination and transportation of photon-induce charge carriers, we have also determined the fluorescence spectra of ZnO nanopowder as a possible fingerprint to ease the comparison with other reported samples [30].

2. Materials and methods

2.1. Experimental procedure

Zinc acetate dihydrate, $Zn(Ac)_2 \cdot 2H_2O$, with 99.9% purity was obtained from Merck. 1-buthanol was used as received from Sigma without further purification.

ZnO synthesis was done as described in [31]. Briefly, 2.1950g $Zn(Ac)_2 \cdot 2H_2O$ were solved in 25 mL 1-buthanol and heated under magnetic stirring. The temperature was 117ºC, the boiling point of 1-buthanol. The higher temperature allowed a shorter reaction time, 6 hours.

2.2. Experimental techniques

Electron microscope images.

The transmission electron images were obtained on dried, finely powdered samples using a Tecnai G2F30 S-TWIN high resolution transmission electron microscope from FEI, operated at an acceleration voltage of 300 kV obtained from a Schottky field emitter with a TEM point resolution of 2Å and line resolution of 1.02 Å.

***X-ray diffraction*.**

X-ray powder diffraction patterns were obtained with a Shimadzu XRD6000 diffractometer, using CuKα (1.5406 Å) radiation operating with 30 mA and 40 kV in the 2θ range 10–70º. A scan rate of 1º min^{-1} was employed.

Thermal analysis.

Thermal behavior of the final ZnO nanopowder was followed by TG-DSC with a Netzsch TG 449C STA Jupiter. The sample was placed in alumina crucible and heated with10 K min^{-1} from room temperature to 900ºC, under the flow of 50 mL min^{-1} dried air.

***Photoluminescence spectrum*.**

Photoluminescence spectrum (PL) was measured with a Perkin Elmer P55 spectrometer using a Xe lamp as a UV light source at ambient temperature, in the range 350–600 nm, with the sample dried and finely powdered. The measurement was made with a scan speed of 200 nm min^{-1}, slit of 10 nm, and cut-off filter of 1%. An excitation wavelength of 320 nm was used.

Diffuse reflectance spectra measurements were made with a JASCO V560 spectrophotometer with solid sample accessory, in the domain 200–800 nm, with a speed of 200 nm min^{-1}.

Photocatalytic activity was determined against four dyes: methylene blue (MB) 10^{-3}% solution, methyl orange (MO) $2 \cdot 10^{-3}$% solution, gentian violet (GV) $0.5 \cdot 10^{-3}$% solution and rhodamine B (Rh) $1.197 \cdot 10^{-3}$% solution by irradiation with

a fluorescent lamp of 160W / 2900 lux, placed at 20 cm distance. Samples of 0.0250 g powder were inserted in 20 mL solution of each dye. At defined time intervals a sample of 3mL was put in a quartz 10 mm cuvette, and its UV-Vis spectra was recorded.

For qualitative antimicrobial assay, the tested bacterial strains were inoculate on solid agar medium in Petri dishes and drops with volume of 5 μL of a 10 mg/mL ZnO suspension were added as spots at equal distances. The Petri dishes were incubated 24h at 37ºC and after that inhibition diameters were assessed.

For quantitative assay, minimum inhibitory concentrations (MICs) of tested ZnO nanopowder were assessed using a binary dilution method. Briefly, 5mg/mL ZnO suspension was added to the first well of each row and after that with a micropipette were obtained 12 binary dilutions, so that last well has a concentration of $2.441406 \cdot 10^{-3}$ mg/mL. In each well were added 15 μL microbial suspension of *E. coli*, *Salmonella*, *S. aureus* and *P. aeruginosa* respectively, with a density of 0.5 McFarland. Plates were incubated for 24 h at 37ºC. After the incubation period, MICs were established by measuring the absorbance (620 nm), using a lab spectrophotometer. All experiments were performed in triplicate and repeated on at least three separate occasions.

3. Results and discussions

The thermal analysis of the resulting white powder was used to monitor the synthesis of ZnO nanopowder. The results are presented in Fig. 1.

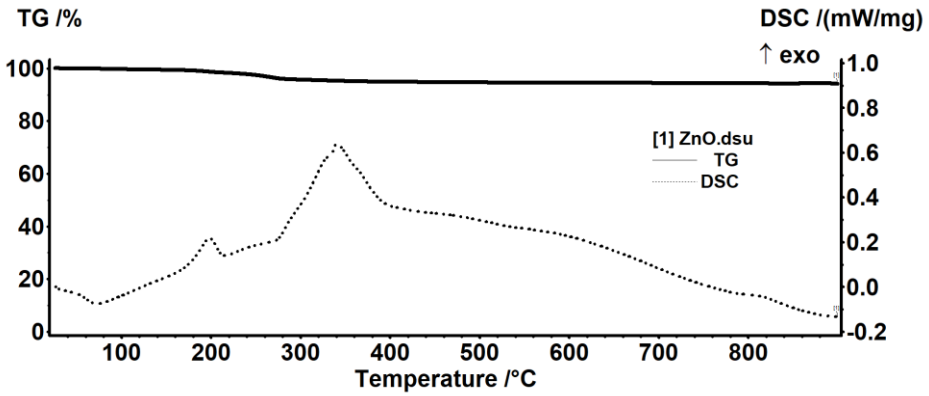

Fig. 1. The TG-DSC curves for ZnO sample obtained by forced hydrolysis in 1-buthanol

Table 1

Thermal analysis data

Temperature interval	RT-150°C	150-280°C	280-410°C	410-900°C
Mass loss	0.63%	3.42%	1.14%	0.62%
DSC Peak	73.1°C	198.9°C	340.4°C	-
Enthalpy (area)	-18.04 J/g	14.17 J/g	132.9 J/g	-

The obtained powder is losing 5.81% of initial mass when heated up to 900°C, in three processes. At low temperature the physically weak bonded solvent molecules are removed in an endothermic process, while at higher temperatures there are two exothermic processes in which strong bonded solvent molecules and some acetate impurities are burned. The numerical data from thermal analysis are presented in table 1.

In order to determine the cristalinity and presence of ZnO, the sample was investigated by X-ray diffraction. The XRD pattern for the nanopowder, Fig. 2, has indicated the formation of single-phase compound. The pattern can be indexed to a hexagonal wurtzite structure [ASTM 80-0075]. The crystallite size of the samples can be estimated from the Scherrer equation, $D = 0.89 \cdot \lambda / \beta \cdot \cos\Theta$, where D is the average grain size, λ is the X-ray wavelength (0.15405 nm), Θ and β are the diffraction angle and FWHM of an observed peak, respectively. The strongest peak (101) at $2\Theta = 36.27^{o}$ was used to calculate the average crystallite size (D) of ZnO particles. The estimated average crystallite size was 18.5 nm.

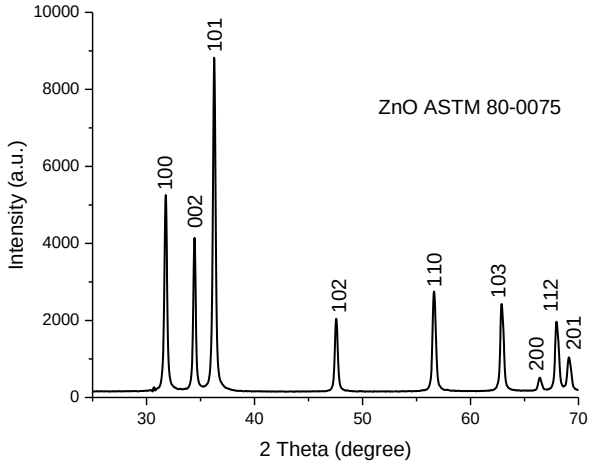

Fig. 2. XRD pattern of the ZnO sample

The TEM bright field image, Fig. 3a, obtained on ZnO reveals that the powder is composed from polyhedral shaped particles, with an average particle size of approximately 20 nm. By correlating the TEM and the XRD information,

as crystallite size is roughly equal with the nanoparticles size, we can conclude that every nanoparticle is a monocrystal. The nanopowder presents a low tendency to form soft agglomerates.

The HRTEM image, Fig. 3b, shows clear lattice fringes of interplanar distances of d = 2.60 Å for nanocrystalline ZnO, corresponding to Miller indices of (0 0 2) crystallographic planes of hexagonal ZnO. In addition, the regular succession of the atomic planes indicates that the nanocrystallites are structurally uniform and crystalline with almost no amorphous phase present. The histogram of the particle size distribution for the ZnO sample indicates a mode value of 20 nm (Fig. 4).

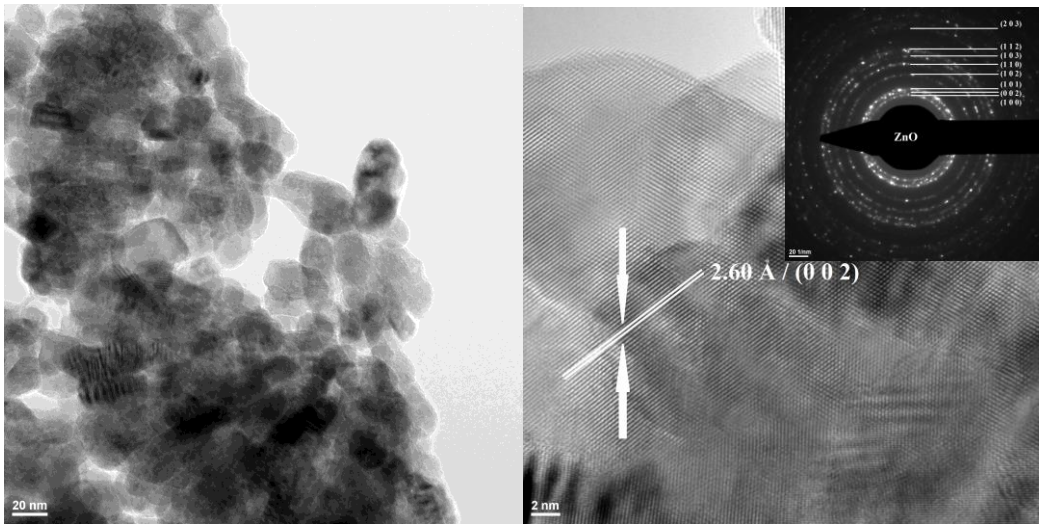

Fig. 3. TEM (a) and HRTEM (b) images and SAED pattern of ZnO particles

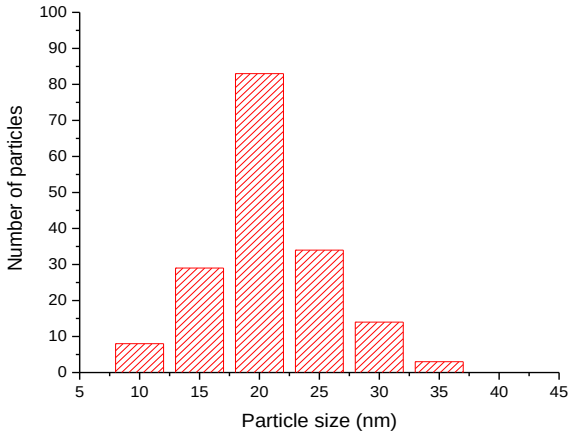

Fig. 4. Particle size distribution histogram for ZnO sample

The sample has a narrow, homogeneous particle size, with more than 85% of them measuring between 15 and 25 nm.

In the photoluminescence spectrum of the as-synthesized ZnO sample (Fig. 5a) there are two regions, one at about 400 nm (near ultraviolet) and 440-530 nm (blue-green), respectively. The ZnO presents a weak UV emission band at 399 nm, corresponding to the near band-edge emission (NBE).

The four other emission bands at 457, 480, and 515-524 nm in the blue-green range are defect-related emissions, indicating a high concentration of surface defects, as expected for polyhedral shape particles. The 480 nm band is relatively common for semiconductor oxides like MIn_2O_4 (M = Ca, Sr, Ba) or SnO_2 confirming that it is caused by the oxygen related defects.

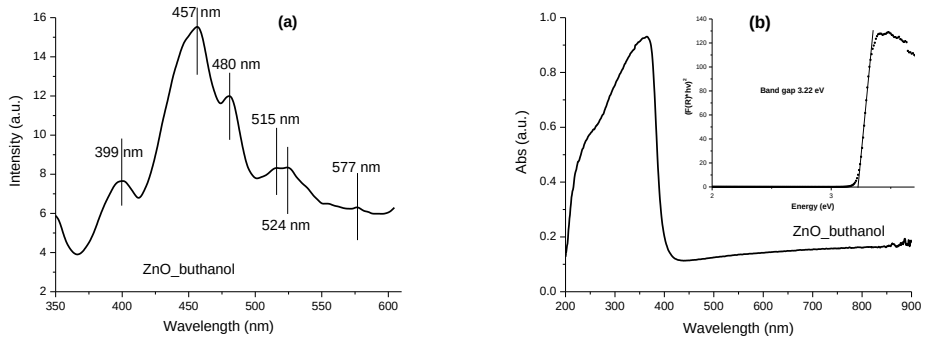

Fig. 5. Photoluminescence (a) and UV-Vis (b) spectra of ZnO nanopowder

The electronic spectrum recorded for the ZnO powder is presented in Fig. 5b. The band gap energy value was calculated by Kubelka-Munk plot to a value of 3.225 eV, in good agreement with the literature. The maximum absorbance for the sample is at 365nm.

The results of photocatalytic activity are presented in Fig. 6.

For diluted solutions the reactions exhibit apparent first-order kinetics, ln(C0/C) = kt, where C0 is the initial concentration of the dye, C is the concentration of dye at time t (min) and *k* is the rate constant of the apparent first order.

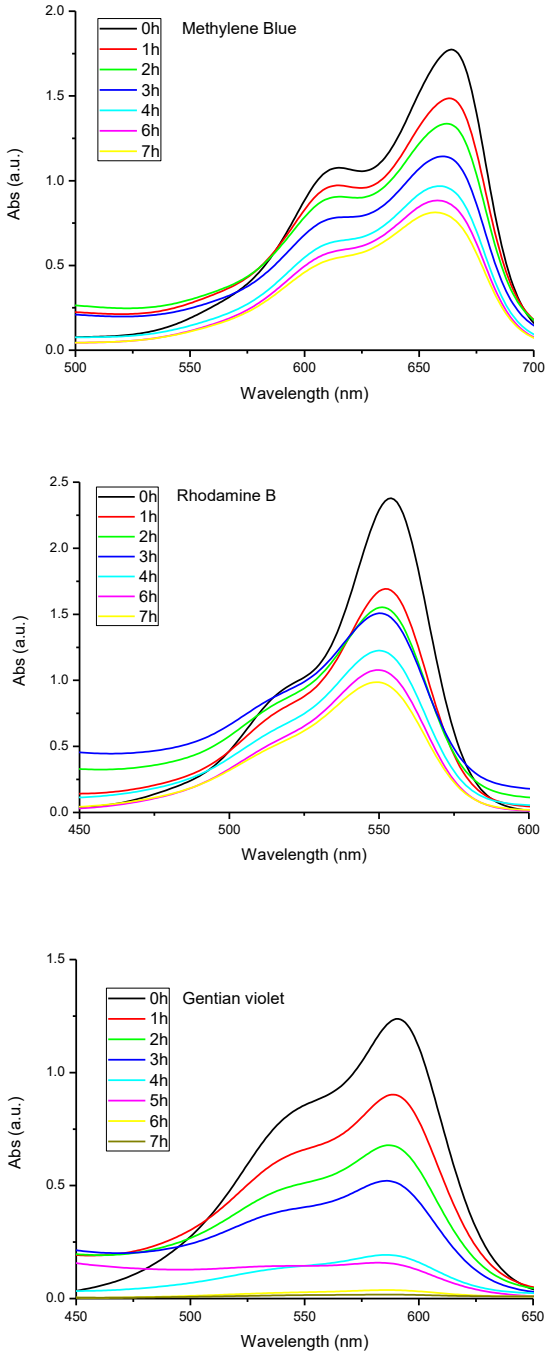

Fig. 6. Photocatalysis activity: methylene blue solution (a); rhodamine b solution (b); gentian violet (c);

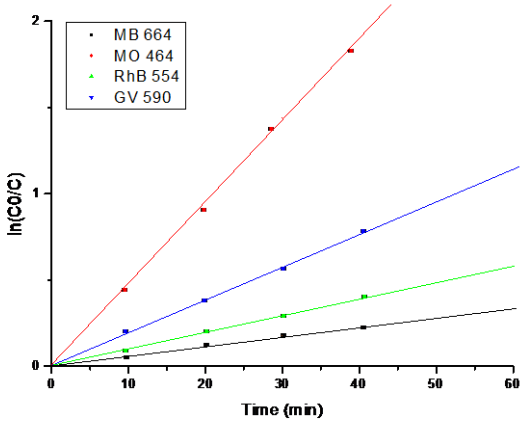

Fig. 6. Photocatalysis activity: determination of the rate constant *k* (d).

The control samples (only dye solutions) indicate that direct photodecomposition of colorants does not occur.

The determination of the rate constant, *k*, was done by plotting the ln(C0/C) versus time (Fig. 6d). The values are presented in table 2.

Table 2

Calculated rate constant value for each dye solution

Dye	Methyl orange	Gentian violet	Rhodamine B	Methylene blue
Rate constant value (*k*) $*10^{-3}$	47.97	22.56	9.11	5.91

For MB solution we can observe a decrease of both 614 and 664 nm absorption peaks, indicating that bot monomer and dimer are decomposed by ZnO nanoparticles. Nevertheless, the photocatalytic activity against MB presented the lowest value from the tested solutions, without being a low value *per se*. The best photocatalytic activity was found against MO solution, with a rate constant that is eight time higher than the one for MB and more than double versus the calculated value for GV, which was on second place. The results indicate that a careful pick of the dye used as model pollutant in photocatalysis studies must be done in order to obtain results that can be compared across different substances or even for same compound [32].

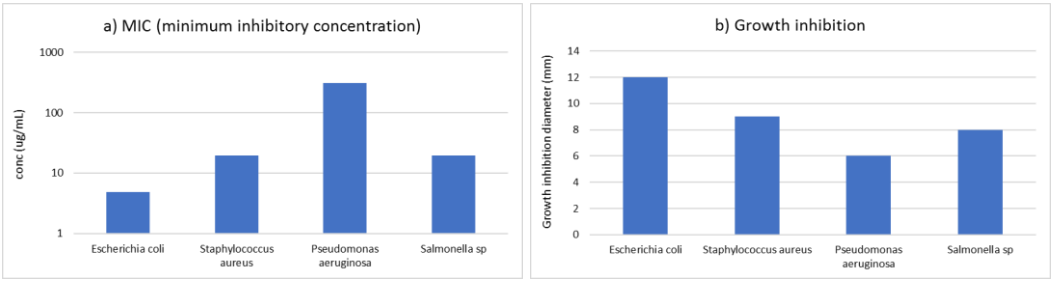

Fig. 7. The antimicrobial assay: minimum inhibitory concentration (a); growth inhibition diameter (b).

The antimicrobial assay, presented in Fig. 7, demonstrates that the ZnO nanoparticles has a good antibacterial activity, especially against Gram-negative strains (*E. coli* and *Salmonella*), but with some noticeable results even on the Gram-positive strain (*S. aureus*). Even if *P. aeruginosa* is a Gram-negative bacterium, the poor results against it might be indicate a native resistance to ZnO action mechanisms (it is also known for its low antibiotic susceptibility).

6. Conclusions

In conclusion, we are presenting for the first time to our knowledge a comparative study of photocatalytic activity for ZnO nanoparticles on four of the most used colorants: methyl orange, methylene blue, rhodamine B and gentian violet. The photocatalytic activity against MO solution was eight time higher than the values recorded for MB solution. This may help researchers understand that a low value obtained against MB is not a particular bad result while a low activity against MO solution may indicate in fact the lack of photocatalysis. The photoluminescence spectrum for ZnO was also recorded to help comparison among various ZnO samples. The antimicrobial assay indicates also a good activity against all strains, except *P. aeruginosa.*

Acknowledgement

This work was supported by a grant of the Romanian Ministry of Research and Innovation, CCCDI - UEFISCDI, project number PN-III-P1-1.2-PCCDI-2017-0689 /P1. „*Lib2Life - Revitalizarea bibliotecilor si a patrimoniului cultural prin tehnologii avansate*” within PNCDI III

R E F E R E N C E S

[1] *M. D. Serb, P. Muller, R. Trusca, O. Oprea, and F. Dumitru*, 'Study of Thermal Decomposition of a Zinc(Ii) Monomethyl Terephthalate Complex, [Zn(Ch3o-Co-C6h4coo)(2)(Oh2)(3)]Center Dot 2h(2)O', *J Therm Anal Calorim*, **vol. 121**, 2015, pp. 691-695.

[2] *O. R. Vasile, E. Andronescu, C. Ghitulica, B. S. Vasile, O. Oprea, E. Vasile, and R. Trusca*, 'Synthesis and Characterization of Nanostructured Zinc Oxide Particles Synthesized by the Pyrosol Method', *J Nanopart Res*, **vol. 14**, 2012, pp.
[3] *O. Oprea, O. R. Vasile, G. Voicu, and E. Andronescu*, 'The Influence of the Thermal Treatment on Luminescence Properties of Zno', *Dig J Nanomater Bios*, **vol. 8**, 2013, pp. 747-756.
[4] *O. Oprea, O. Ciocirlan, A. Badanoiu, and E. Vasile*, 'Synthesis and Characterization of Zno Nanostructures Obtained in Mixtures of Ionic Liquids with Organic Solvents', *Cent Eur J Chem*, **vol. 12**, 2014, pp. 749-756.
[5] *O. Oprea, O. R. Vasile, G. Voicu, L. Craciun, and E. Andronescu*, 'Photoluminescence, Magnetic Properties and Photocatalytic Activity of Gd3+ Doped Zno Nanoparticles', *Dig J Nanomater Bios*, **vol. 7**, 2012, pp. 1757-1766.
[6] *G. Voicu, O. Oprea, B. S. Vasile, and E. Andronescu*, 'Antibacterial Activity of Zinc Oxide - Gentamicin Hybrid Material', *Dig J Nanomater Bios*, **vol. 8**, 2013, pp. 1191-1203.
[7] *M. Radulescu, S. Popescu, D. Ficai, M. Sonmez, O. Oprea, A. Spoiala, A. Ficai, and E. Andronescu*, 'Advances in Drug Delivery Systems, from 0 to 3d Superstructures', *Curr Drug Targets*, **vol. 19**, 2018, pp. 393-405.
[8] *D. Ficai, O. Oprea, A. Ficai, and A. M. Holban*, 'Metal Oxide Nanoparticles: Potential Uses in Biomedical Applications', *Curr Proteomics*, **vol. 11**, 2014, pp. 139-149.
[9] *F. Vaja, C. Comanescu, O. Oprea, D. Ficai, and C. Guran*, 'Effects of Zno Nanoparticles on the Wet Scrub Resistance and Photocatalytic Properties of Acrylic Coatings', *Rev Chim-Bucharest*, **vol. 63**, 2012, pp. 722-726.
[10] *B. S. Vasile, O. Oprea, G. Voicu, A. Ficai, E. Andronescu, A. Teodorescu, and A. Holban*, 'Synthesis and Characterization of a Novel Controlled Release Zinc Oxide/Gentamicin-Chitosan Composite with Potential Applications in Wounds Care', *Int J Pharmaceut*, **vol. 463**, 2014, pp. 161-169.
[11] *E. E. Totu, C. M. Cristache, E. Voicila, O. Oprea, I. Agir, O. Tavukcuoglu, and A. C. Didilescu*, 'On Physical and Chemical Characteristics of Poly(Methylmethacrylate) Nanocomposites for Dental Applications. I', *Mater Plast*, **vol. 54**, 2017, pp. 666-672.
[12] *F. Vaja, D. Ficai, A. Ficai, O. Oprea, and C. Guran*, 'Multifunctional Advanced Coatings Based on Zno/M Obtained by Nanocasting Method', *J Optoelectron Adv M*, **vol. 15**, 2013, pp. 107-113.
[13] *G. Niculae, N. Badea, A. Meghea, O. Oprea, and I. Lacatusu*, 'Coencapsulation of Butyl-Methoxydibenzoylmethane and Octocrylene into Lipid Nanocarriers: Uv Performance, Photostability and in Vitro Release', *Photochem Photobiol*, **vol. 89**, 2013, pp. 1085-1094.
[14] *I. Lacatusu, L. V. Arsenie, G. Badea, O. Popa, O. Oprea, and N. Badea*, 'New Cosmetic Formulations with Broad Photoprotective and Antioxidative Activities Designed by Amaranth and Pumpkin Seed Oils Nanocarriers', *Ind Crop Prod*, **vol. 123**, 2018, pp. 424-433.
[15] *O. Oprea, E. Andronescu, D. Ficai, A. Ficai, F. N. Oktar, and M. Yetmez*, 'Zno Applications and Challenges', *Curr Org Chem*, **vol. 18**, 2014, pp. 192-203.
[16] *I. Lacatusu, N. Badea, A. Murariu, O. Oprea, D. Bojin, and A. Meghea*, 'Antioxidant Activity of Solid Lipid Nanoparticles Loaded with Umbelliferone', *Soft Mater*, **vol. 11**, 2013, pp. 75-84.
[17] *G. Voicu, O. Oprea, B. S. Vasile, and E. Andronescu*, 'Photoluminescence and Photocatalytic Activity of Mn-Doped Zno Nanoparticles', *Dig J Nanomater Bios*, **vol. 8**, 2013, pp. 667-675.
[18] *M. Radulescu, L. V. Arsenie, O. Oprea, and B. S. Vasile*, 'Optical and Photocatalytic Properties of Copper(Ii) Doped Zinc Oxide', *Rev Chim-Bucharest*, **vol. 67**, 2016, pp. 2596-2599.
[19] *D. Gingasu, O. Oprea, I. Mindru, D. C. Culita, and L. Patron*, 'Alkali Earth Metal Indates Synthesized by Precursor Method', *Dig J Nanomater Bios*, **vol. 6**, 2011, pp. 1215-1226.
[20] *D. C. Culita, C. M. Simonescu, R. E. Patescu, M. Dragne, N. Stanica, and O. Oprea*, 'O-Vanillin Functionalized Mesoporous Silica - Coated Magnetite Nanoparticles for Efficient Removal of Pb(Ii) from Water', *J Solid State Chem*, **vol. 238**, 2016, pp. 311-320.
[21] *N. E. Mousa, C. M. Simonescu, R. E. Patescu, C. Onose, C. Tardei, D. C. Culita, O. Oprea, D. Patroi, and V. Lavric*, 'Pb2+ Removal from Aqueous Synthetic Solutions by Calcium Alginate and Chitosan Coated Calcium Alginate', *React Funct Polym*, **vol. 109**, 2016, pp. 137-150.

[22] *D. C. Culita, C. M. Simonescu, M. Dragne, N. Stanica, C. Munteanu, S. Preda, and O. Oprea*, 'Effect of Surfactant Concentration on Textural, Morphological and Magnetic Properties of Cofe2o4 Nanoparticles and Evaluation of Their Adsorptive Capacity for Pb(Ii) Ions', *Ceram Int*, **vol. 41**, 2015, pp. 13553-13560.

[23] *A. V. Zanfir, G. Voicu, A. I. Badanoiu, D. Gogan, O. Oprea, and E. Vasile*, 'Synthesis and Characterization of Titania-Silica Fume Composites and Their Influence on the Strength of Self-Cleaning Mortar', *Compos Part B-Eng*, **vol. 140**, 2018, pp. 157-163.

[24] *D. C. Culita, L. Dyakova, G. Marinescu, T. Zhivkova, R. Spasov, L. Patron, R. Alexandrova, and O. Oprea*, 'Synthesis, Characterization and Cytotoxic Activity of Co(Ii), Ni(Ii), Cu(Ii), and Zn(Ii) Complexes with Nonsteroidal Antiinflamatory Drug Isoxicam as Ligand', *J Inorg Organomet P*, **vol. 29**, 2019, pp. 580-591.

[25] *D. Gingasu, I. Mindru, L. Patron, A. Ianculescu, E. Vasile, G. Marinescu, S. Preda, L. Diamandescu, O. Oprea, M. Popa, C. Saviuc, and M. C. Chifiriuc*, 'Synthesis and Characterization of Chitosan-Coated Cobalt Ferrite Nanoparticles and Their Antimicrobial Activity', *J Inorg Organomet P*, **vol. 28**, 2018, pp. 1932-1941.

[26] *G. Badea, A. G. Bors, I. Lacatusu, O. Oprea, C. Ungureanu, R. Stan, and A. Meghea*, 'Influence of Basil Oil Extract on the Antioxidant and Antifungal Activities of Nanostructured Carriers Loaded with Nystatin', *Cr Chim*, **vol. 18**, 2015, pp. 668-677.

[27] *B. S. Vasile, O. R. Vasile, D. C. Ghitulica, F. C. Ilie, I. F. Nicoara, R. Trusca, O. C. Oprea, V. A. Surdu, and I. A. Neacsu*, 'Eu3+-Doped Zno Nanostructures: Advanced Characterizations, Photoluminescence and Cytotoxic Effect', *Rom J Morphol Embryo*, **vol. 58**, 2017, pp. 941-952.

[28] *M. Radulescu, D. Ficai, O. Oprea, A. Ficai, E. Andronescu, and A. M. Holban*, 'Antimicrobial Chitosan Based Formulations with Impact on Different Biomedical Applications', *Curr Pharm Biotechno*, **vol. 16**, 2015, pp. 128-136.

[29] *O. R. Vasile, I. Serdaru, E. Andronescu, R. Trusca, V. A. Surdu, O. Oprea, A. Ilie, and B. S. Vasile*, 'Influence of the Size and the Morphology of Zno Nanoparticles on Cell Viability', *Cr Chim*, **vol. 18**, 2015, pp. 1335-1343.

[30] *L. Zhang, H. Wu, Y. Jin, H. Sun, D. Liu, Y. Lv, G. Ju, L. Chen, and Y. Hu*, 'Competition of Luminescence and Photocatalysis in Melilite: Recombination and Transportation of Electrons', *Physica B*, **vol. 573**, 2019, pp. 87-91.

[31] *O. Oprea, E. Andronescu, B. S. Vasile, G. Voicu, and C. Covaliu*, 'Synthesis and Characterization of Zno Nanopowder by Non-Basic Route', *Dig J Nanomater Bios*, **vol. 6**, 2011, pp. 1393-1401.

[32] *I. Mindru, D. Gingasu, L. Patron, G. Marinescu, J. M. Calderon-Moreno, S. Preda, O. Oprea, and S. Nita*, 'Copper Aluminate Spinel by Soft Chemical Routes', *Ceram Int*, **vol. 42**, 2016, pp. 154-164.